RAA 2016 Vol. **16** No. **10**, 152 (6pp) doi: 10.1088/1674–4527/16/10/152
http://www.raa-journal.org *http://iopscience.iop.org/raa*

***R**esearch in*
***A**stronomy and*
***A**strophysics*

The γ-ray emission produced by protons that escape from supernova remnant G349.7+0.2

Xiao Zhang[1], Hui Li[2] and Yang Chen[1,3]

[1] School of Astronomy and Space Science, Nanjing University, Nanjing 210023, China
[2] Department of Astronomy, University of Michigan, 500 Church Street, Ann Arbor, MI 48109, USA
[3] Key Laboratory of Modern Astronomy and Astrophysics, Nanjing University, Ministry of Education, Nanjing 210023, China; *ygchen@nju.edu.cn*

Received 2016 May 13; accepted 2016 May 27

Abstract G349.7+0.2 is an interacting supernova remnant (SNR) expanding in a dense medium. Recently, a very strong γ-ray source coincident with this SNR has been revealed by *Fermi*-LAT and H.E.S.S. observations which shows a broken power-law-like spectrum. An escaping-diffusion model, including the power-law and δ-function injection, is applied to this source which can naturally explain the spectral feature in both the GeV and TeV regime. We use the Markov Chain Monte Carlo method to constrain the model parameters and find that the correction factor of slow diffusion around this SNR, $\chi \sim 0.01$ for power-law injection and $\chi \sim 0.1$ for δ-function injection, can fit the data best with reasonable molecular cloud mass. This slow diffusion is also consistent with previous results from both phenomenological models and theoretical predication.

Key words: radiation mechanisms: non-thermal — ISM: individual objects (G349.7+0.2) — ISM: supernova remnants — gamma-rays: ISM

1 INTRODUCTION

The origin of Galactic cosmic rays (CRs) has puzzled scientists for more than a century since their discovery in 1912 by Victor Hess. In the last few decades, the supernova remnant (SNR) paradigm of the origin of CR particles with energy up to the 'knee' $\sim 3 \times 10^{15}$ eV through diffusive shock acceleration (DSA) has been widely discussed (see e.g. Hillas 2005, for reviews). The discovery of SNRs' radio continuum spectra, as well as non-thermal X-ray emission, provides solid evidence for electron acceleration at the SNR shock. The evidence for proton acceleration can be tested by hadronic γ-ray emission which comes from the decay of neutral pions generated in proton–proton collisions. Because molecular clouds (MCs) can provide a number of targets bombarded by relativistic protons, the hadronic γ-ray emission can be enhanced significantly around the so-called interacting SNRs whose shock wave comes into contact with nearby MCs. Indeed, statistical studies show that most of the detected γ-ray-bright SNRs can be classified into this group (e.g., Hewitt et al. 2009, 2013). In particular, the characteristic pion-decay γ-ray signal was detected in two interacting SNRs, IC 443 (Ackermann et al. 2013) and W44 (Giuliani et al. 2011; Ackermann et al. 2013; Cardillo et al. 2014), providing strong evidence of proton acceleration.

G349.7+0.2 is a thermal composite SNR (Chen & Slane 2003; Ergin et al. 2015), and its interaction with dense MCs/clumps had already been confirmed by the detection of five OH (1720 MHz) masers towards the center of the SNR (Frail et al. 1996) and line emissions from several molecular transitions (Reynoso & Mangum 2000; Dubner et al. 2004; Lazendic et al. 2010) and the ground state transition of ortho-water (Rho et al. 2015). The distance to this source was first estimated as $d \sim 22$ kpc based on observations of H I (Caswell et al. 1975), 1720 MHz OH masers (Frail et al. 1996) and CO (Reynoso & Mangum 2000). Recently, it was revised to $d \sim 11.5$ kpc by Tian & Leahy (2014) according to updated knowledge of kinematics in the inner Galaxy. At this distance, the radio angular size of $\sim 2.5'$ in diameter gives a physical radius of $R_{\rm age} \sim 4$ pc. In combination with the shock velocity $\sim 710\ {\rm km\,s^{-1}}$ (Lazendic et al. 2005) and the number density of the ambient medium $\sim 10\ {\rm cm^{-3}}$ (Tian & Leahy 2014), the dynamical age and explosion energy can be estimated as $t_{\rm age} \sim 2.4$ kyr and $E_{\rm SN} \sim 6 \times 10^{50}$ erg according to the Sedov solution, respectively.

In radio observations, G349.7+0.2 is a shell-type SNR with enhancements at the eastern and southern parts, and has a spectral index of -0.47 ± 0.06 (Shaver et al. 1985). In X-rays, it was first detected by ASCA (Yamauchi et al. 1998), presenting a similar shape with radio morphology. The analysis of ASCA (Slane et al. 2002) and *Chandra*

observations (Lazendic et al. 2005) showed that the spectrum is dominated by the thermal component. In the GeV and TeV energy regime, a γ-ray source coincident with G349.7+0.2 was reported by Castro & Slane (2010) based on *Fermi*-LAT observations and by Abramowski et al. (2015) based on H.E.S.S. observations, respectively.

With respect to the origin of the γ-ray emission, Abramowski et al. (2015) strongly disfavor the leptonic origin and support the hadronic-dominated scenario in which the proton distribution has a broken power-law form, although the single power-law distribution with a high energy exponential cutoff cannot be statistically ruled out. Before the publication of the TeV data, an accumulated escaping-diffusion model was developed to explain the γ-ray emission of nine interacting SNRs including G349.7+0.2, and the predicted TeV spectrum for this source is consistent with the H.E.S.S. observation (Li & Chen 2012).

In this paper, based on updated γ-ray data in both GeV and TeV bands, we applied the escaping-diffusion model, including two kinds of injection processes, to explain the γ-ray data and used the Markov Chain Monte Carlo (MCMC) method to constrain the model parameters.

2 MODEL DESCRIPTION

In the escaping-diffusion model, the energetic protons that escape from the expanding SNR shock front diffuse into the ambient ISM and collide with nearby MCs, generating hadronic γ-rays. The γ-ray emission comes from every point inside an MC which has a finite volume and a constant density, and the total emissivity can be obtained by integrating over the volume of the MC. At a given point inside the MC, the energetic protons are a collection of the diffusive protons escaping from different shock radius as the SNR expands. Like in Li & Chen (2012), we also approximate the MC as a truncated cone that subtends a solid angle Ω at the SNR center and has thickness $\Delta R_{\rm c}$ with inner radius L_1 and outer radius L_2 ($\Delta R_{\rm c} = L_2 - L_1$). Therefore, for the case of an interacting SNR-MC system ($L_1 = R_{\rm age}$), the mean distribution of protons in the MCs at the SNR age $t_{\rm age}$ is

$$F_{\rm ave}(E_{\rm p}, t_{\rm age}) = \int_{R_{\rm age}}^{R_{\rm age}+\Delta R_{\rm c}} f(E_{\rm p}, R, t_{\rm age}) \cdot R^2 {\rm d}R \Big/ \int_{R_{\rm age}}^{R_{\rm age}+\Delta R_{\rm c}} R^2 {\rm d}R, \quad (1)$$

where $E_{\rm p}$ and R are the proton energy and the distance to the SNR center, respectively, and the function f can be derived via solving the diffusion equation which is written as

$$\frac{\partial}{\partial t} f(E_{\rm p}, R, t) = \frac{D(E_{\rm p})}{R^2}\frac{\partial}{\partial R} R^2 \frac{\partial}{\partial R} f(E_{\rm p}, R, t) + Q(E_{\rm p}, R, t), \quad (2)$$

where $D(E_{\rm p}) = 10^{28}\chi(E_{\rm p}/10\,{\rm GeV})^{\delta}\ {\rm cm^2\,s^{-1}}$ (χ and δ are the correction factor for slow diffusion and the index of diffusion coefficient respectively) is the diffusion coefficient, and $Q(E_{\rm p}, R, t)$ is the source term. In this paper, we consider two kinds of injections: (a) at any given time, the distribution of protons that escape from the shock front has a power-law form (e.g. Aharonian & Atoyan 1996; Torres et al. 2008; Li & Chen 2010); (b) it is a δ-function (e.g. Gabici et al. 2009; Ellison & Bykov 2011; Ohira et al. 2011).

2.1 The Power-law Case

In this case, referred to as Model A, all of the protons ($E_{\rm p,min} < E_{\rm p} < E_{\rm p,max}$) can continuously escape from the expanding shock surface at any time. Thus the source term is $Q = Q_0 E_{\rm p}^{-p}\delta[R - R_{\rm s}(t)]/4\pi R^2$, where p is the proton index, $R_s(t)$ is the shock radius, and Q_0 is the normalization and is determined by $t_{\rm age}\int E_{\rm p} Q_0 E_{\rm p}^{-p}{\rm d}E_{\rm p} = \eta E_{\rm SN}$ (η is the fraction of explosion energy converted into protons). Then, the diffusion Equation (2) can be solved as (Zhang & Chen 2016)

$$f(E_{\rm p}, R, t) = \int_0^t \frac{Q_0 E_{\rm p}^{-p}}{4\pi^{3/2} R_{\rm d} R_s(t_i) R} \left\{ \exp\left[-\left(\frac{R - R_s(t_i)}{R_{\rm d}} \right)^2 \right] - \exp\left[-\left(\frac{R + R_s(t_i)}{R_{\rm d}} \right)^2 \right] \right\} {\rm d}t_i, \quad (3)$$

where $R_{\rm d} = \sqrt{4D(t - t_i)}$.

The solid lines in the top panel of Figure 1 show the average distribution of escaping protons given by Equations (1) and (3) for different $\Delta R_{\rm c}$. Here we assume an SNR with $t_{\rm age} = 10^4$ yr, $R_{\rm age} = 12.5$ pc, $n_0 = 1\ {\rm cm^{-3}}$ and $E_{\rm SN} = 10^{51}$. The values of other parameters are $\chi = 0.01$, $p = 2.0$, $\delta = 0.5$, $\eta = 10\%$ and $E_{\rm p,max} = E_{\rm knee}$, where $E_{\rm knee} = 3$ PeV is the CR knee energy. As a comparison, the point-like continuous injection (namely $f(E_{\rm p}, R, t)$, given by eq. (8) in Aharonian & Atoyan 1996 and referred to as Model A$^-$) is also displayed by the dashed lines in the same panel. Only considering the volume of the MC (the dashed lines), the spectrum of the escaping protons has a low-energy cutoff above which the slope is close to $p + \delta$. The average spectrum of the escaping protons in the MC will then assume the form of a broken power-law when the volume of both the source and the MC are taken into account (the solid lines). Above the break energy, the slope is also close to $p + \delta$; while below that break, the slope depends on the thickness of the MC $\Delta R_{\rm c}$ in addition to the parameters p and δ.

2.2 The δ-function case

In this escaping model (Model B), at a given time t, only the protons with the maximum energy $E_{\rm p,max}(t)$ can escape from the acceleration site at a diffusion length $\kappa(E_{\rm p,max})/V_{\rm s} = L_{\rm FEB}$ ahead of the SNR shock, where $\kappa(E_{\rm p,max})$ is the diffusion coefficient in the upstream re-

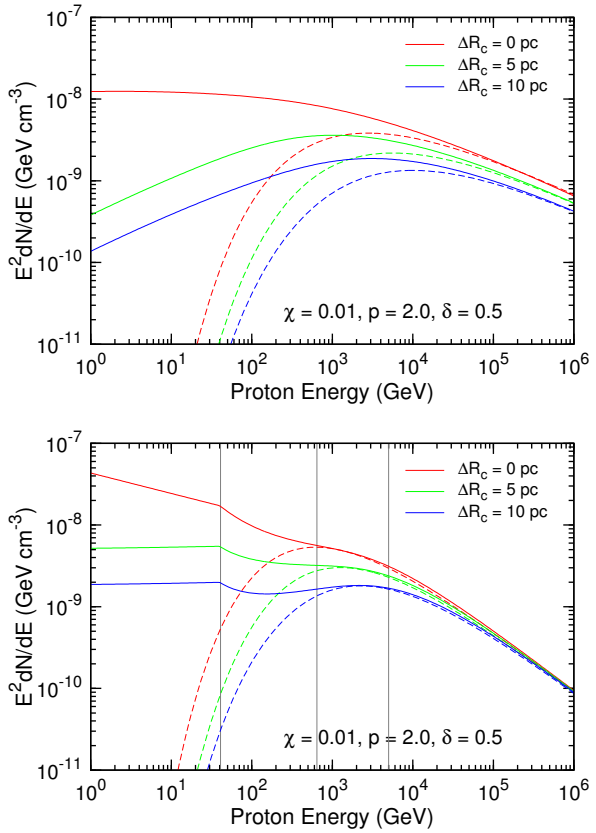

Fig. 1 The mean distribution of runaway protons in MC at the SNR age $t_{\rm age} = 10^4$ yr ($R_{\rm age} = 12.5$ pc for $E_{\rm SN} = 10^{51}$ erg and $n_0 = 1$ cm^{-3}) for different values of the MC thickness, $\Delta R_{\rm c} =$ 0 pc (*red*), 5 pc (*green*) and 10 pc (*blue*). *Top*: The solid and dashed lines correspond to Model A and Model A$^-$, respectively. *Bottom*: The solid and dashed lines represent Model B and Model B$^-$, respectively. The three vertical lines correspond to the break energy given in Fig. 2.

gions that are very close to the shock, $V_{\rm s}$ is the shock velocity, and $L_{\rm FEB}$ is the so-called free escape boundary and is set as $L_{\rm FEB} = f_{\rm s}R_{\rm s}$ ($f_{\rm s}$ is a numerical factor, e.g. Ptuskin & Zirakashvili 2005; Ellison & Bykov 2011). Given $\kappa(E_{\rm p,max})$, therefore, the maximum energy can be determined by the condition $\kappa(E_{\rm p,max})/V_{\rm s} = f_{\rm s}R_{\rm s}$. However, the diffusion coefficient around the shock strongly depends on the level of magnetic turbulence generated by the accelerated particles themselves. This makes the problem nonlinear and very difficult to solve. Although the non-linear theory has been widely discussed and studied, there are still some uncertainties in some aspects of the problem, including the nature of CR-driven instability and wave damping (e.g. Bell & Lucek 2001; Vladimirov et al. 2006).

For simplicity, here we adopt a phenomenological approach to parameterize the maximum energy, namely, $E_{\rm p,max} = E_{\rm knee}(t/t_{\rm sed})^{-s}$, where the index s is obtained according to the assumption that protons with energy $\sim$1 GeV can escape at the end of the Sedov phase (Gabici et al. 2009). Moreover, we also assume that protons with energy $E_{\rm p}$ escape at the free escape boundary, namely, from the spherical surface at radius $R_{\rm esc} = (1 + f_{\rm s})R_{\rm s}$. However, we do not consider the diffusion effect in the regions from the shock to the free escape boundary, which will slightly soften the proton spectrum (Ohira et al. 2010). For the SNR-MC system, however, there are some differences: once the CRs encounter the MC, they all are expected to escape from the SNR due to the strong ion-neutral damping (e.g. Ohira et al. 2011). Thus, the escape radius is $R_{\rm esc}(E_{\rm p}) = \min[(1+f_{\rm s})R_{\rm s}, L_1]$, which will give a break at $E_{\rm br,1} = [L_1/((1 + f_{\rm s})R_{\rm sed})]^{-5s/2}$. Below this break energy, the protons escape at almost the same time. In combination with the Sedov solution, we have

$$t_{\rm esc}(E_{\rm p}) = \begin{cases} t_{\rm sed}\left(\frac{E_{\rm p}}{E_{\rm knee}}\right)^{-1/s}, & E_{\rm p} > E_{\rm br,1}, \\ t_{\rm sed}\left[\frac{L_1}{(1+f_{\rm s})R_{\rm sed}}\right]^{5/2}, & E_{\rm p} < E_{\rm br,1}. \end{cases} \quad (4)$$

$$R_{\rm esc}(E_{\rm p}) = \begin{cases} (1 + f_{\rm s})R_{\rm sed}\left(\frac{E_{\rm p}}{E_{\rm knee}}\right)^{-2/5s}, & E_{\rm p} > E_{\rm br,1}, \\ L_1, & E_{\rm p} < E_{\rm br,1}. \end{cases} \quad (5)$$

Thus the source term is $Q = \frac{N_0 E_{\rm p}^{-p}}{4\pi R^2}\delta[R - R_{\rm esc}(E)]\delta[t - t_{\rm esc}(E)]$. Then the distribution of the runaway CRs can be derived as (Ohira et al. 2011)

$$f_{\rm d}(E_{\rm p}, R, t) = \frac{N_0 E_{\rm p}^{-p}}{4\pi^{3/2}R_{\rm dif,d}R_{\rm esc}R} \left\{\exp\left[-\left(\frac{R - R_{\rm esc}}{R_{\rm dif,d}}\right)^2\right] - \exp\left[-\left(\frac{R + R_{\rm esc}}{R_{\rm dif,d}}\right)^2\right]\right\}, \quad (6)$$

where $R_{\rm dif,d} = \sqrt{4D(t - t_{\rm esc})}$. As pointed out by Ohira et al. (2011), this solution has a break $E_{\rm br,e}$ given by the condition $R_{\rm esc}(E_{\rm br,e}) = R_{\rm dif,d}(E_{\rm br,e})$. Moreover, it is close to the case of point-like impulsive injection (eq. (3) in Aharonian & Atoyan 1996) as $R_{\rm esc} \to 0$ or $R \gg R_{\rm esc}$.

Taking the volume of the MC into account, there is another energy break $E_{\rm br,2}$ given by the condition $L_2 = R_{\rm dif,d}(E_{\rm br,2}) + R_{\rm esc}(E_{\rm br,2})$[1]. An example of the three break energies is shown in Figure 2. Besides the value of the parameters given in Model A, we take $f_{\rm s} = 0.1$ (Ellison & Bykov 2011) and $s = 3.0$ which correspond to the end time of the Sedov phase $t_{\rm rad} = 2.9 \times 10^4$ yr (Blondin et al. 1998). It is important to note that the relation $E_{\rm br,1} < E_{\rm br,e} < E_{\rm br,2}$ shown in Figure 2 is not always valid as pointed out by Ohira et al. (2011). For example, one can have $E_{\rm br,e} < E_{\rm br,1}/E_{\rm br,2}$ if χ is large enough or $E_{\rm br,2} < E_{\rm br,1}/E_{\rm br,e}$ if $t_{\rm age}$ is small enough.

The mean distributions of runaway CRs in an MC are shown in the bottom panel of Figure 1. As a comparison, the point-like impulsive injection (namely $f(E_{\rm p}, R, t)$,

[1] Generally speaking, the condition $L_1 = R_{\rm dif,d} + R_{\rm esc}$ can give another break energy $E_{\rm cut}$ below which a proton cannot effectively reach the MC. However, this condition vanishes for the interacting SNR-MC system because all protons can reach the MC after considering the wave damping caused by the ion-neutral interaction.

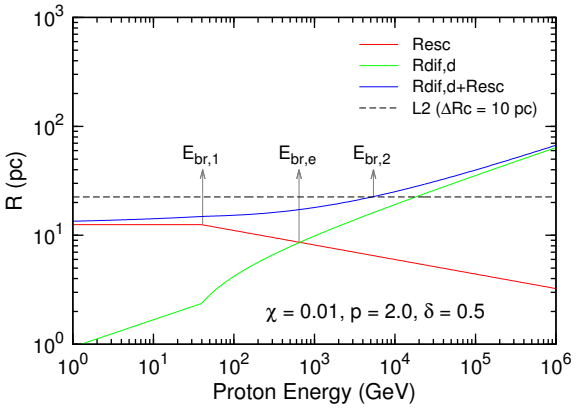

Fig. 2 The escaping radius $R_{\rm esc}$, the diffusion length $R_{\rm dif,d}$ and their sum vary with the proton energy at the SNR age $t_{\rm age} = 10^4$ yr ($R_{\rm age} = 12.5$ pc for $E_{\rm SN} = 10^{51}$ erg and $n_0 = 1$ cm^{-3}). The three arrows mark the three break energies in model B for $\chi = 0.01$, $p = 2.0$, $\delta = 0.5$ and $\Delta R_{\rm c} = 10$ pc.

given by eq. (2) in Aharonian & Atoyan 1996 and referred to as Model B$^-$) is also plotted by the dashed lines in the same panel. The break energy $E_{\rm br,e}$ can be seen for $\Delta R_{\rm c} \to 0$ (red lines) but can be erased by the MC thickness for the case of $E_{\rm br,e} < E_{\rm br,2}$. Above the energy max$[E_{\rm br,1}, E_{\rm br,e}, E_{\rm br,2}]$, the distribution is close to the point-like impulsive injection case and the slope is close to $p + 3\delta/2$. But below the energy min$[E_{\rm br,1}, E_{\rm br,e}, E_{\rm br,2}]$, the proton distribution is the same as that produced by shock.

Finally, once the mean distribution of the runaway CRs is obtained, the expected γ-ray flux from the entire MC is

$$F_\gamma = \frac{M_{\rm cl}}{m_{\rm p}} \frac{q_\gamma(F_{\rm ave})}{4\pi d^2}, \qquad (7)$$

where $M_{\rm cl}$ and $m_{\rm p}$ are the MC mass and proton mass, respectively; $q_\gamma(F_{\rm ave})$ is the emissivity per atom and is calculated according to the analytic method developed by Kelner et al. (2006), including the enhancement factor of 1.84 due to contribution from heavy nuclei (Mori 2009).

3 THE MCMC FITTING AND RESULTS

We now apply the escaping-diffusion model to SNR G349.7+0.2 with properties: $t_{\rm age} = 2.4 \times 10^3$ yr, $E_{\rm SN} = 6 \times 10^{50}$ erg, $n_0 = 10$ cm^{-3} and $d = 11.5$ kpc and take model parameters: $\eta = 10\%$ and $f_{\rm s} = 0.1$. Besides these fixed parameters, there are still five parameters in total, including p, δ, χ, $\Delta R_{\rm c}$ and $M_{\rm cl}$, that need to be determined. To constrain these model parameters, the MCMC technique is employed here. This approach is a very efficient way to explore the model parameter space and obtains the best-fitted parameters, especially for high dimensions. A brief introduction to the basic procedure of MCMC sampling applied to γ-ray spectral fit can be found in Fan et al. (2010) and Yuan et al. (2011). More details about the MCMC method can be found in Neal (1993), Gamerman (1997) and Mackay (2003).

If all of the above five parameters in our model are set free in the MCMC routine, then some of them do not converge very well for both Model A and Model B. One possible reason may be that the updated observed data still cannot well constrain the model parameters. For example, the GeV-TeV data have a broken power-law form but the the break energy cannot be well confined with large 1σ error, $E_{\gamma,\rm bre} = 55^{+70}_{-30}$ GeV (Abramowski et al. 2015). The current spectral features, e.g., flux and spectral shape, are not adequate to fully determine all the model parameters with high precision. Additional prior information based on realistic physical conditions of CR acceleration and propagation is needed.

Therefore, instead of changing the correction factor of slow diffusion, χ, continuously, we only allow it to have three different values, $\chi = 0.1$, 0.01 and 0.001. We also give the prior distribution range $\delta \sim 0.3$–0.7 (Berezinskii et al. 1990) for the power-law index of the diffusion coefficient. In addition, the upper limits are taken away from the data in our fitting process. The best-fitted parameters are listed in Table 1 and the best-fit spectral energy distributions (SEDs) are displayed in Figure 3, which can give a satisfactory fitting to the data. For Model A, due to the similar SEDs for the three sets of parameters, we only plot the result for $\chi = 0.01$ in the top panel of Figure 3. But for Model B, due to the variation in relative values of the three break energies, the spectral shape for the three cases has little difference with each other, see the bottom panel in Figure 3.

4 DISCUSSION AND CONCLUSIONS

In the above fitting process, we try to fit the observational data by using three different values for χ and obtain three sets of best-fitting model parameters. The parameter p and δ have no remarkable change because they are mainly determined by the slope of γ-ray spectra above the break energy.

From Table 1, the fitted spectral index of protons is obviously greater than 2.0, which is inconsistent with the predication from the standard DSA for strong shocks. A possible reason for this is that when the shock is expanding in a partially-ionized medium, the population of hot neutrals generated via charge exchange immediately behind the shock will produce the so-called neutral return flux. Such a neutral return flux will heat up the upstream gas, leading to the formation of a neutral-induced precursor, and thus reduces the fluid compression ratio $r < 4$ which determines the spectral index of accelerated particles $p = (r + 2)/(r - 1)$ (Blasi et al. 2012; Morlino & Gabici 2015). This effect is expected to be important at SNR shock velocity $v_{\rm sh} \leq 3000\,{\rm km\,s^{-1}}$ and large neutral fraction. These conditions seem to be met for this interacting SNR with velocity $\sim 700\,{\rm km\,s^{-1}}$.

From the ^{12}CO data, the total mass of associated clouds is reported by Dubner et al. (2004) and is estimated

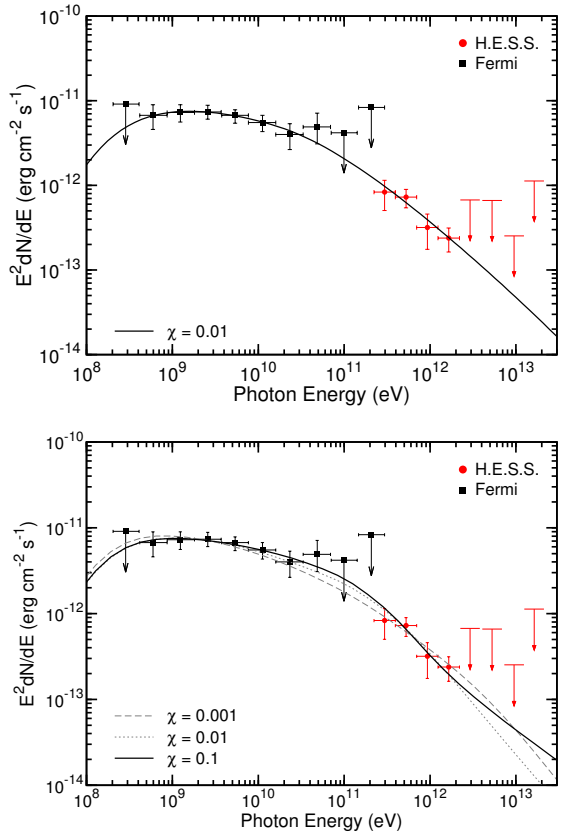

Fig. 3 Best-fit SED derived from observations (Abramowski et al. 2015) for Model A (*top*) and Model B (*bottom*). The corresponding model parameters are listed in Table 1.

to be $\sim 5 \times 10^3 M_\odot$ given the distance of 11.5 kpc. This is very close to the fitted results for $\chi = 0.01$ in Model A and for $\chi = 0.1$ in Model B. The other two options for χ in Model A will either over- or under-estimate the cloud mass. But in Model B, the fitted MC mass for $\chi = 0.01$ also seems to be acceptable compared with observation. For both models, we try to fix $M_{\rm cl} = 5 \times 10^3 M_\odot$ instead of the χ with three different values. We find that the parameters cannot be well converged in Model A, implying that $M_{\rm cl}$ is not the key parameter for determining the spectral shape in this case. In Model B, however, we can obtain $\chi = 0.13^{+0.15}_{-0.11}$ ($p = 2.0^{+0.2}_{-0.2}$, $\delta = 0.44^{+0.26}_{-0.14}$, $\Delta R_{\rm c} < 3.4$ pc) with large 1σ error, which means that the model parameters except for the MC thickness $\Delta R_{\rm c}$ can be well constrained if they have more data with energy greater than $\sim$10 TeV (see the bottom panel of Fig. 3).

In both models, the correction factor for slow diffusion favored by the CO observations is consistent with the results reported by other authors (e.g., Fujita et al. 2009; Giuliani et al. 2010; Gabici et al. 2010; Li & Chen 2012; Tang & Chevalier 2015). This slow diffusion around SNR seems to be a common phenomenon. The physical reason may be that the Alfvén waves excited by the CR streaming instability can strongly scatter the particles, and thus suppress the diffusion coefficient (e.g., Fujita et al. 2010).

Table 1 Fitting Parameters with 1σ Errors or 95% Upper Limits

Model	χ	$\alpha_{\rm p}$	δ	$\Delta R_{\rm c}$ (pc)	$M_{\rm cl}(10^4 M_\odot)$
A	0.1	$2.2^{+0.3}_{-0.2}$	$0.70^{-}_{-0.25}$	$12.8^{+14.7}_{-7.7}$	$3.8^{+15.6}_{-2.8}$
	0.01	$2.3^{+0.2}_{-0.3}$	$0.66^{+0.03}_{-0.30}$	$5.3^{+6.1}_{-4.7}$	$0.7^{+2.8}_{-0.5}$
	0.001	$2.0^{+0.3}_{-}$	$0.70^{-}_{-0.25}$	≤ 0.3	$0.06^{+0.01}_{-0.04}$
B	0.1	$2.0^{+0.3}_{-0.3}$	$0.50^{+0.20}_{-0.20}$	≤ 4.9	$0.54^{+2.2}_{-0.3}$
	0.01	$2.2^{+0.2}_{-0.3}$	$0.63^{+0.07}_{-0.22}$	$1.6^{+3.2}_{-1.6}$	$0.18^{+0.6}_{-0.1}$
	0.001	$2.3^{+0.2}_{-0.2}$	$0.70^{-}_{-0.40}$	$0.7^{+1.4}_{-0.5}$	$0.06^{+0.2}_{-0.04}$

Besides the escaping-diffusion model, there is another type of model, referred to as the "crushed cloud" model, for the interacting SNRs to explain γ-ray emission (e.g. Uchiyama et al. 2010; Tang & Chevalier 2015). In these models, the π^0-decay γ-rays are from the direct collision between accelerated protons and shock-crushed dense clouds without the diffusion process. Thus, to explain the observed soft γ-ray spectrum with a spectral break around several GeV, the protons accelerated by the SNR shock should have a broken power-law form and the proton index above the break should be close to $\sim$3. Several physical processes, e.g., Alfvén damping caused by ion-neutral collision (Malkov et al. 2011) and two-step acceleration (Inoue et al. 2010), were proposed and can steepen the particle spectrum by about one power $\Delta p \sim 1$. For SNR G349.7+0.2, it can be seen that, based on the the Bayesian Information Criterion (BIC), the broken power law model with $\Delta p = 0.5$ and $\Delta p = 1.0$ gives equally good fits to the γ-ray data and are statistically compatible with the power-law with exponential cutoff model (Abramowski et al. 2015). As a comparison, we also calculate $\rm BIC_{dif}$ of Model A for $\chi = 0.01$ and Model B for $\chi = 0.1$ and find that $\Delta{\rm BIC} = {\rm BIC} - {\rm BIC_{dif}}$ can slightly exceed the value of 2 except for $\Delta p = 0.5$.

In conclusion, whatever injection model we adopt, the escaping-diffusion model applied to SNR G349.7+0.2 can naturally produce the γ-ray spectral features without assuming that the accelerated protons should have a broken power-law form. The fitted results for $\chi \sim 0.01$ in Model A and for $\chi \sim 0.1$ in Model B are consistent with the CO observations and can provide a good fit to the γ-ray data.

Acknowledgements We thank the support of the National Natural Science Foundation of China (Grant No. 11233001), 973 Program (Grant 2015CB857100), the Educational Ministry of China (Grant 20120091110048) and the program B for Outstanding PhD candidate of Nanjing University.

References

Abramowski, A., Aharonian, F., Ait Benkhali, F., et al. (H.E.S.S. Collaboration) 2015, A&A, 574, A100

Ackermann, M., Ajello, M., Allafort, A., et al. 2013, Science, 339, 807
Aharonian, F. A., & Atoyan, A. M. 1996, A&A, 309, 917
Bell, A. R., & Lucek, S. G. 2001, MNRAS, 321, 433
Berezinskii, V. S., Bulanov, S. V., Dogiel, V. A., & Ptuskin, V. S. 1990, Astrophysics of Cosmic Rays (Amsterdam: North-Holland)
Blasi, P., Morlino, G., Bandiera, R., Amato, E., & Caprioli, D. 2012, ApJ, 755, 121
Blondin, J. M., Wright, E. B., Borkowski, K. J., & Reynolds, S. P. 1998, ApJ, 500, 342
Cardillo, M., Tavani, M., Giuliani, A., et al. 2014, A&A, 565, A74
Castro, D., & Slane, P. 2010, ApJ, 717, 372
Caswell, J. L., Clark, D. H., & Crawford, D. F. 1975, Australian Journal of Physics Astrophysical Supplement, 37, 39
Chen, Y., & Slane, P. 2003, in Astronomical Society of the Pacific Conference Series, 289, The Proceedings of the IAU 8th Asian-Pacific Regional Meeting, Volume 1, eds. S. Ikeuchi, J. Hearnshaw, & T. Hanawa, 295
Dubner, G., Giacani, E., Reynoso, E., & Parón, S. 2004, A&A, 426, 201
Ellison, D. C., & Bykov, A. M. 2011, ApJ, 731, 87
Ergin, T., Sezer, A., Saha, L., et al. 2015, ApJ, 804, 124
Fan, Z. H., Liu, S. M., Yuan, Q., & Fletcher, L. 2010, A&A, 517, L4
Frail, D. A., Goss, W. M., Reynoso, E. M., et al. 1996, AJ, 111, 1651
Fujita, Y., Ohira, Y., & Takahara, F. 2010, ApJ, 712, L153
Fujita, Y., Ohira, Y., Tanaka, S. J., & Takahara, F. 2009, ApJ, 707, L179
Gabici, S., Aharonian, F. A., & Casanova, S. 2009, MNRAS, 396, 1629
Gabici, S., Casanova, S., Aharonian, F. A., & Rowell, G. 2010, in SF2A-2010: Proceedings of the Annual meeting of the French Society of Astronomy and Astrophysics, eds. S. Boissier, M. Heydari-Malayeri, R. Samadi, & D. Valls-Gabaud, 313
Gamerman, D. 1997, Markov Chain Monte Carlo: Stochastic Simulation for Bayesian Inference (London: Chapman and Hall)
Giuliani, A., Tavani, M., Bulgarelli, A., et al. 2010, A&A, 516, L11
Giuliani, A., Cardillo, M., Tavani, M., et al. 2011, ApJ, 742, L30
Hewitt, J. W., Acero, F., Brandt, T. J., et al. 2013, arXiv:1307.6570
Hewitt, J. W., Yusef-Zadeh, F., & Wardle, M. 2009, ApJ, 706, L270
Hillas, A. M. 2005, Journal of Physics G Nuclear Physics, 31, R95
Inoue, T., Yamazaki, R., & Inutsuka, S.-i. 2010, ApJ, 723, L108
Kelner, S. R., Aharonian, F. A., & Bugayov, V. V. 2006, Phys. Rev. D, 74, 034018
Lazendic, J. S., Slane, P. O., Hughes, J. P., Chen, Y., & Dame, T. M. 2005, ApJ, 618, 733
Lazendic, J. S., Wardle, M., Whiteoak, J. B., Burton, M. G., & Green, A. J. 2010, MNRAS, 409, 371
Li, H., & Chen, Y. 2010, MNRAS, 409, L35
Li, H., & Chen, Y. 2012, MNRAS, 421, 935
Mackay, D. J. C. 2003, Information Theory, Inference and Learning Algorithms (Cambridge: Cambridge University Press)
Malkov, M. A., Diamond, P. H., & Sagdeev, R. Z. 2011, Nature Communications, 2, 194
Morlino, G., & Gabici, S. 2015, MNRAS, 451, L100
Neal, R. M. 1993, Probabilistic Inference Using Markov Chain Monte Carlo Methods (Department of Computer Science, University of Toronto, Canada)
Ohira, Y., Murase, K., & Yamazaki, R. 2010, A&A, 513, A17
Ohira, Y., Murase, K., & Yamazaki, R. 2011, MNRAS, 410, 1577
Ptuskin, V. S., & Zirakashvili, V. N. 2005, A&A, 429, 755
Reynoso, E. M., & Mangum, J. G. 2000, ApJ, 545, 874
Rho, J., Hewitt, J. W., Boogert, A., Kaufman, M., & Gusdorf, A. 2015, ApJ, 812, 44
Shaver, P. A., Salter, C. J., Patnaik, A. R., van Gorkom, J. H., & Hunt, G. C. 1985, Nature, 313, 113
Slane, P., Chen, Y., Lazendic, J. S., & Hughes, J. P. 2002, ApJ, 580, 904
Tang, X., & Chevalier, R. A. 2015, ApJ, 800, 103
Tian, W. W., & Leahy, D. A. 2014, ApJ, 783, L2
Torres, D. F., Rodriguez Marrero, A. Y., & de Cea Del Pozo, E. 2008, MNRAS, 387, L59
Uchiyama, Y., Blandford, R. D., Funk, S., Tajima, H., & Tanaka, T. 2010, ApJ, 723, L122
Vladimirov, A., Ellison, D. C., & Bykov, A. 2006, ApJ, 652, 1246
Yamauchi, S., Koyama, K., Kinugasa, K., et al. 1998, Astronomische Nachrichten, 319, 111
Yuan, Q., Liu, S., Fan, Z., Bi, X., & Fryer, C. L. 2011, ApJ, 735, 120
Zhang, X., & Chen, Y. 2016, ApJ, 821, 43